SCIENCE CHINA
Earth Sciences

SPECIAL TOPIC: The Severe Fog and Haze Event over Eastern China in January 2013
• RESEARCH PAPER •

January 2014 Vol.57 No.1: 14–25
doi: 10.1007/s11430-013-4773-4

Mechanism for the formation of the January 2013 heavy haze pollution episode over central and eastern China

WANG YueSi*, YAO Li, WANG LiLi, LIU ZiRui†, JI DongSheng, TANG GuiQian, ZHANG JunKe, SUN Yang, HU Bo & XIN JinYuan

State Key Laboratory of Atmospheric Boundary Layer Physics and Atmospheric Chemistry (LAPC), Institute of Atmospheric Physics, Chinese Academy of Sciences, Beijing 100029, China

Received August 12, 2013; accepted October 28, 2013; published online November 27, 2013

In January 2013, a long-lasting episode of severe haze occurred in central and eastern China, and it attracted attention from all sectors of society. The process and evolution of haze pollution episodes were observed by the "Forming Mechanism and Control Strategies of Haze in China" group using an intensive aerosol and trace gases campaign that simultaneously obtained data at 11 ground-based observing sites in the CARE-China network. The characteristics and formation mechanism of haze pollution episodes were discussed. Five haze pollution episodes were identified in the Beijing-Tianjin-Hebei (Jing-Jin-Ji) area; the two most severe episodes occurred during 9–15 January and 25–31 January. During these two haze pollution episodes, the maximum hourly $PM_{2.5}$ mass concentrations in Beijing were 680 and 530 μg m^{-3}, respectively. The process and evolution of haze pollution episodes in other major cities in the Jing-Jin-Ji area, such as Shijiazhuang and Tianjin were almost the same as those observed in Beijing. The external cause of the severe haze episodes was the unusual atmospheric circulation, the depression of strong cold air activities and the very unfavorable dispersion due to geographical and meteorological conditions. However, the internal cause was the quick secondary transformation of primary gaseous pollutants to secondary aerosols, which contributed to the "explosive growth" and "sustained growth" of $PM_{2.5}$. Particularly, the abnormally high amount of nitric oxide (NO_x) in the haze episodes, produced by fossil fuel combustion and vehicle emissions, played a direct or indirect role in the quick secondary transformation of coal-burning sulphur dioxide (SO_2) to sulphate aerosols. Furthermore, gaseous pollutants were transformed into secondary aerosols through heterogeneous reactions on the surface of fine particles, which can change the particle's size and chemical composition. Consequently, the proportion of secondary inorganic ions, such as sulphate and nitrate, gradually increased, which enhances particle hygroscopicity and thereby accelerating formation of the haze pollution.

haze pollution episode, meteorology, air pollution complex, cooperative transition, Jing-Jin-Ji

Citation: Wang Y S, Yao L, Wang L L, et al. 2014. Mechanism for the formation of the January 2013 heavy haze pollution episode over central and eastern China. Science China: Earth Sciences, 57: 14−25, doi: 10.1007/s11430-013-4773-4

Air pollution in China exhibited noticeable changes over the past 30 years, changing from point-source pollution in the 1980s to urban pollution in the 1990s. Since the start of the century, air pollution has become more regional and complex (Chan and Yao, 2008). Rapid economic development and urbanization have resulted in a large amount of pollutants being emitted into the atmosphere. China's energy consumption increased 120% from 2000 to 2010. Coal accounted for most of the primary energy consumption (up to 70%), which is much higher than the coal consumption in developed countries (20% to 30%). The vast majority of coal consumption was concentrated in the haze pollution regions of northern China, central China and eastern China (Department of Energy Statistics, National Bureau of Statistics of China, 2001; 2011). In these areas, the coexistence of

*Corresponding author (email: wys@dq.cern.ac.cn)
†Corresponding author (email: lzr@dq.cern.ac.cn)

numerous air pollutants with high concentrations and the complicated interactions among them lead to the formation of an air pollution complex and haze. For example, haze occurrence frequency (number of days on which haze occurred) is greater than 50% in Beijing and Shanghai and greater than 30% in Guangzhou and Shenzhen (Chang et al., 2009; Che et al., 2009). The air pollution complex is characterized by an increase in the oxidizing capacity of the atmosphere, reduced atmospheric visibility and the deterioration of environmental quality throughout the entire region; essentially, the air pollution complex features the interactions between the sources and sinks of the air pollutants, the coupling processes of the transformation of pollutants, and the synergetic environmental impacts of the air pollutants (Ding and Zhu, 2003; Zhu et al., 2005; Zhang et al., 2008; Parrish and Zhu, 2009). In an air pollution complex, the coexistence of high concentrations of primary and secondary gaseous and particulate pollutants provide a large amount of reactants for heterogeneous reactions on the surface of fine particles. These reactions change the oxidizing capacity of the atmosphere and the chemical compositions and physicochemical and optical properties of particulate matter, therefore, the formation of the air pollution complex and gray haze is accelerated (Zhu et al., 2010). As one of the most important compositions of fine particles, the formation mechanism of sulphate has attracted much attention. In recent field studies, large amounts of sulphate were discovered to accompany mineral particles, but the formation mechanism was still unknown (Zhang et al., 2003; Sullivan et al., 2007). A few laboratory simulation studies observed that SO_2 alone cannot transform into sulphate at the surface of the mineral particles without Fe_2O_3 and MgO. The coexistence of O_3 is able to promote the conversion of SO_2 to sulphate (Usher et al., 2003). Even so, the surface reaction mechanism of SO_2 on the mineral particles under different atmospheric conditions and its contribution to the gas-solid reaction of SO_2 in the troposphere are not yet completely understood.

In January 2013, a long-lasting severe haze episode occurred in central and eastern China. Based on the CARE-China network (Campaign on the atmospheric Aerosol REsearch net-work of China), supported by the Strategic Priority Research Program Grant of the Chinese Academy of Sciences (A and B Category), an intensive aerosol and trace gases campaign was simultaneously performed by the "Forming Mechanism and Control Strategies of Haze in China" group at 11 ground-based observing sites during the regional haze pollution episode. The external causes of the large scope and long duration of the haze, such as synoptic processes, the atmospheric circulation and the regional meteorological conditions were analyzed. Furthermore, the characteristics of the haze pollution episodes and their formation mechanism were analyzed by considering the hourly changes of $PM_{2.5}$ aerosols and their chemical compositions in Beijing, a megacity in the Jing-Jin-Ji area. These observations and analyses provide a general picture of the process and evolution of the haze pollution episodes in January 2013 in central and eastern China. The improved CARE-China network provides a suitable research platform for scientists to help prevent and control haze pollution over the next 20-30 years.

1 Experiment and methods

1.1 Site description

The observation sites in this study were located in central and eastern China, and distributed mainly in the Jing-Jin-Ji area; 11 of the observation sites were from the CARE-China network (Table 1). Among the 11 sites, six were located in Beijing, Tianjin, Shijiazhuang, Wuxi, Hefei and Changsha, which are the major cities in Jing-Jin-Ji area and the Yangtze River Delta (YRD) region. One site was located in Xianghe, a suburban site located between the two megacities of Beijing and Tianjin. The two county sites were located in Yucheng and Qianyanzhou, which are located in Shandong and Jiangxi provinces, respectively. The two regional background sites were located in Xinglong and Dinghushan, which are considered background areas of Jing-Jin-Ji and the YRD, respectively. An intensive aerosol

Table 1 The geographic information of the CARE-China network

Area	Station Name	Station type	Latitude (N)	Longitude (E)	Altitude (m a.s.l)	*N* (day)
Jing-Jin-Ji	Beijing (BJ)	Northern megacity	116.37°	39.97°	44	31
	Tianjin (TJ)	Northern megacity	117.21°	39.08°	20	29
	Shijiazhuang (SJZ)	Northern megacity	114.53°	38.03°	70	31
	Xianghe (XH)	Northern suburbs	116.96°	39.75°	9	30
	Xinglong (XL)	Northern background	117.58°	40.39°	960	31
Central and eastern	Yucheng (YC)	Northern country	116.37°	36.67°	37	31
	Wuxi (WX)	Eastern city	120.22°	31.40°	60	31
	Hefei (HF)	Eastern city	117.27°	31.86°	70	31
	Changsha (CS)	Central city	113.06°	28.21°	60	27
	Qianyanzhou (QYZ)	Southeast country	115.07°	26.75°	47	31
	Dinghushan (DHS)	Pearl River Delta background	112.5°	23.17°	34	31

and trace gases campaign was performed from 1 January to 31 January 2013. One-month measurements of aerosol mass concentrations and gaseous pollutants at the 11 observation sites were analyzed in this study.

1.2 Observation methods

Observation sites in the CARE-China network were equipped with RP1400-$PM_{2.5}$ or RP1405-$PM_{2.5}$ (Thermo Scientific: http://www.thermoscientic.com), which provide a continuous direct mass measurement of particulates by utilizing a tapered element oscillating microbalance (TEOM) (Patashnick et al., 1991). NO_x was measured using a chemiluminescence NO_x analyser (Model 42I, Thermo-Fisher Scientific, USA), O_3 was measured using a UV photometric O_3 analyzer (Model 49I, Thermo-Fisher Scientific, USA), SO_2 was measured using a pulsed fluorescence SO_2 analyzer (Model 43I, Thermo-Fisher Scientific, USA) and CO was measured with a non-dispersive infrared analyzer (Model 48I, Thermo-Fisher Scientific, USA). The installation, commission and maintenance of the instruments were performed according to the China National Environmental Monitoring Center specification (automated methods for ambient air quality monitoring, 2006), which are described in Xin et al (2012).

The non-refractory submicron (NR-PM_1) aerosol species including organics, sulphate, nitrate, ammonium and chloride were measured using a HR-ToF-AMS at an urban site in Beijing. In the HR-ToF-AMS, an aerodynamic lens is used to sample and focus ambient particles into a narrow beam that is transmitted to a heated surface (~600°C), where particles are flash vaporized upon impact. The resulting vapor molecules are ionized by a 70 eV electron impaction (EI), and then, the positive ions are analyzed using a ToF mass spectrometer. Details of the AMS are available in previous publications (DeCarlo et al., 2006; Canagaratna et al., 2007).

2 Result and discussions

2.1 Concentrations of air pollutants and their spatial distributions

2.1.1 Beijing-Tianjin-Hebei area

An air pollution episode is a state of the ambient air environment in which the concentrations of the air contaminants are elevated to or are in excess of certain defined levels during persistent meteorological conditions. In this study, we defined an air pollution episode as follows: the daily $PM_{2.5}$ mass concentration exceeds Grade II National Ambient Air Quality Standard (75 μg m^{-3}, ambient air quality standards which is to be implemented in 2016: GB3095-2012) for two successive days. According to this definition, five haze pollution episodes occurred in January 2013 in the Jing-Jin-Ji area (Figure 1). The three megacities (i.e., Beijing, Shijiazhuang and Tianjin) in the Jing-Jin-Ji area exhibited consistent development and evolution of the five haze pollution episodes. Note that, Haze Episodes 1, 3 and 4 lasted longer in Shijiazhuang and Tianjin than they did in Beijing. Furthermore, the particle mass concentration in Beijing dropped dramatically (an hourly $PM_{2.5}$ below 50 μg m^{-3}) on 15 January after the dispersion of Haze Episode 2, whereas the particle mass concentrations remained at a high level on 15 January in Shijiazhuang and Tianjin. In these two cities, Haze Episode 3 closely followed Haze Episode 2. Among the five haze pollution episodes, the heaviest pollution day and the most sustained pollution period was observed during Haze Episode 2; the maximum hourly averaged $PM_{2.5}$ in Beijing, Tianjin and Shijiazhuang were 680, 500 and 660 μg m^{-3}, respectively. Beijing and Shijiazhuang were the most polluted cities in the Jing-Jin-Ji area; the air pollution in Tianjin was also severe but less so than those of Beijing and Shijiazhuang.

Figure 1 displays the variation of the gaseous pollutants (NO_x, O_3, SO_2 and CO) in Beijing, Tianjin and Shijiazhuang during the observation period. The average mass concentration of SO_2, NO_x and CO in Beijing were 51, 152 and 2.8 mg m^{-3}, respectively. The average mass concentration of SO_2, NO_x and CO in Tianjin were 111, 111 and 2.4 mg m^{-3}, respectively. The average mass concentration of SO_2, NO_x and CO in Shijiazhuang were 227, 197 and 5.4 mg m^{-3}, respectively. SO_2, NO_x and CO were emitted mainly from the fossil fuel combustion and vehicle emissions in the urban environment. Because of the energy structure adjustment, such as the shift from coal to gas, electric heating and reduced industrial production, the local coal consumption in Beijing was largely reduced. As a result, the SO_2 concentration in Beijing was much lower than that in Tianjin and Shijiazhuang. However, the NO_x concentration in Beijing was still very high because the number of motor vehicles increased rapidly. The air pollution in Shijiazhuang was more severe than that in Beijing and Tianjin. The daily averages of $PM_{2.5}$, SO_2 and NO_x exceeded the Grade II standard in most days of the observation period. Shijiazhuang is located in South-Central Hebei, and is situated on the piedmont plain of the Taihang Mountains. The air pollutants emitted in the piedmont plain usually are accumulated in Shijiazhuang because the air masses move from the southeast and are blocked by the Taihang Mountains. Furthermore, air masses originating from the northwest usually carry dust aerosols: as the air traverses the Taihang Mountains, the dust aerosols are rapidly displayed nearer to the surface, thereby intensifying the air pollution in Shijiazhuang. Dry weather conditions also increased the road and construction dust in Shijiazhuang compared with other cities. Consequently, the contributions of fugitive dust and dust aerosols were more important to particle pollution in Shijiazhuang than in Beijing and Tianjin. The Jing-Jin-Ji region is one of the most densely populated and economically developed areas in China. This area is already heavily burdened with

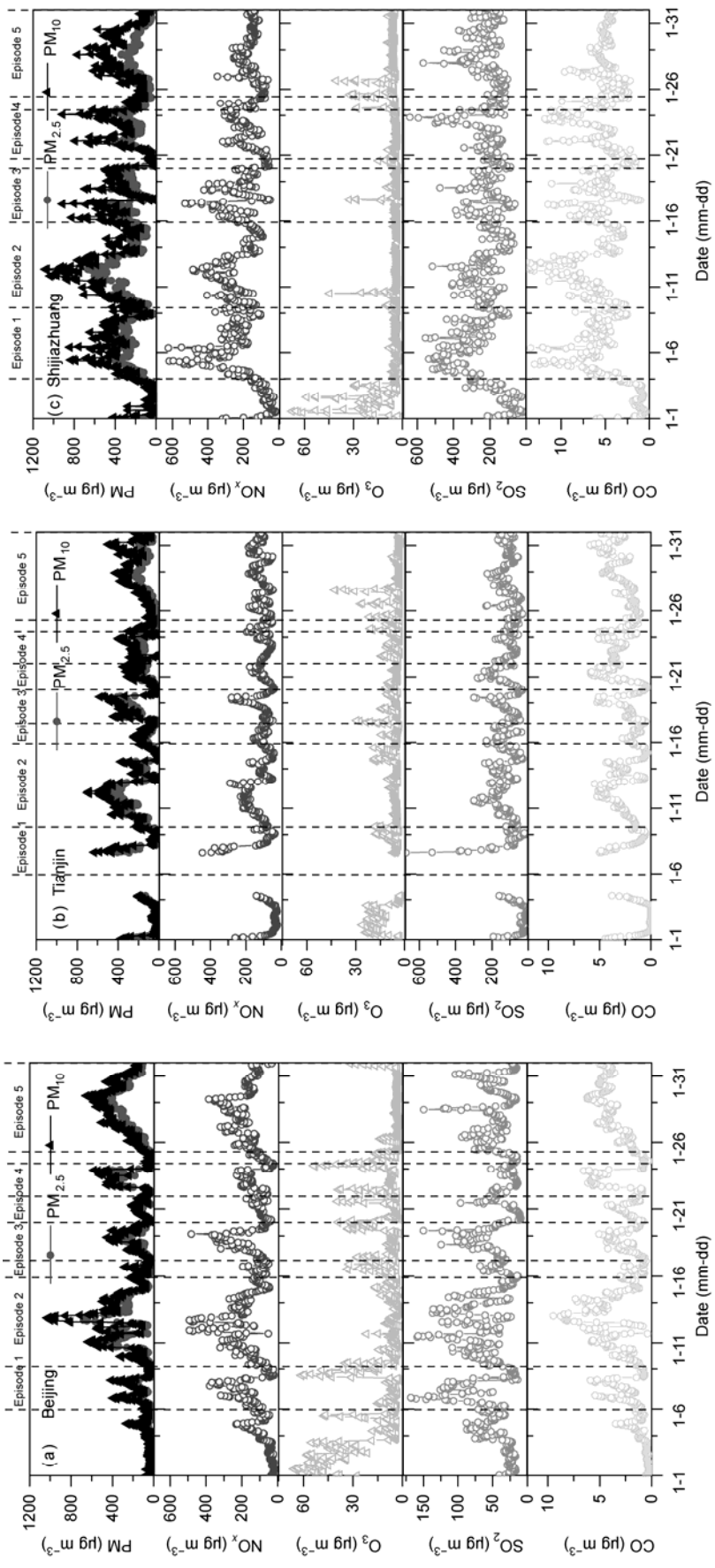

Figure 1 Variation of particle matter and gaseous pollutants in three megacities (Beijing, Tianjin and Shijiazhuang) in January 2013. The five haze episodes are marked between the dote lines.

pollution; the added dust will undoubtedly promote heavy air pollution events if unfavourable weather processes occur that inhibit pollutant dispersion.

2.1.2 Central and eastern China

Table 2 displays the monthly averaged daily concentrations of $PM_{2.5}$ in major cities and regional background sites in central and eastern China. On average, the mass concentration of $PM_{2.5}$ in eastern China and south China was lower than that in the Jing-Jin-Ji region during the observation period. The spatial distribution changes of $PM_{2.5}$ indicate that its concentration gradually decreased from north to south. Specifically, Yucheng's $PM_{2.5}$ exceeded the Grade II standard for 29 days and exceeded the Grade I standard (35 μg m^{-3}) of China for 31 days, with a maximum hourly mass concentration of 700 μg m^{-3}. There were 21 and 25 days when the daily $PM_{2.5}$ mass concentration exceeded the Grade II standard in Wuxi and Hefei (the maximum hourly mass concentrations of $PM_{2.5}$ in both cities exceeded 330 μg m^{-3}). In these two cities, none of the days during the one-month observation period met the Grade I standard.

In Changsha, one of the major cities in Central China, 26 days had a daily $PM_{2.5}$ mass concentration that exceeded the Grade II standard. None of the days during the one-month observation period met the Grade I standard. As an agro-ecological experimental station located in the Jiangxi province, the air pollution levels at the Qianyanzhou station can be considered the regional background concentrations in Central China. During January 2013, in Qianyanzhou, 17 days had daily $PM_{2.5}$ mass concentrations that exceeded the Grade II standard, and only two days met the Grade I standard. As the regional background station of the Pearl River Delta (PRD) region, the air pollution conditions at Dinghushan were poor. Ten days experienced a daily $PM_{2.5}$ mass concentration that exceeded the Grade II standard, and only four days met the Grade I standard. Although the average and maximum mass concentrations of $PM_{2.5}$ in central and eastern China were lower than those in the Jing-Jin-Ji region, the fine particle background concentrations in these two regions were higher. The average mass concentrations of $PM_{2.5}$ at the Qianyanzhou and Dinghushan stations were higher than that at the Xinglong station. Furthermore, 2–5 days experienced a daily $PM_{2.5}$ that met the Grade I standard in the major cities of Jing-Jin-Ji, whereas none of the days met the Grade I standard in the major cities of central and eastern China. In Hefei and Changsha, 81% and 96%, respectively, of the days had a daily $PM_{2.5}$ mass concentration that exceeded the Grade II standard, and these percentages are much higher than those in Beijing and Tianjin. Compared with the Jing-Jin-Ji region, the air pollution in central and eastern China also became increasingly severe. It was more difficult to improve the air quality in central and eastern China because its background pollution was much higher than that in the Jing-Jin-Ji region.

2.2 Atmospheric circulation, meteorological conditions and the structure of boundary layer during heavy haze pollution episodes

2.2.1 Atmospheric circulation

The inhibited dispersion due to geographical and meteorological conditions was the main factor for the heavy and consecutive regional haze pollution episode over much of central and eastern China. The typical weather conditions that contribute to long-term heavy pollution are intense cold air events, weak weather systems, prevailing westerly upper air flow over North China, strong zonal circulation, weak meridional circulation at 500 hPa, warm air advection at 850 hPa during the pollution episode, a weak pressure field over North China (i.e., weak winds), prevailing southly winds over the piedmont plain of the Jing-Jin-Ji region, and persistent stagnant weather. In central and eastern China, a weak pressure field dominated in these regions during 6–7 January and 9–31 January. Although low and high pressure alternated, the entire region was dominated by low or weak pressure due to cold air. The burst of severe cold air in the middle and high latitudes and its southern movement occurred on the 15th and 24th. The pollutants were swept up by a strong northwest wind, but a weak weather system quickly dominated the region. Figure 2 displays the weather

Table 2 Averaged daily concentrations for $PM_{2.5}$ in 11 ground-based observing sites

Station Name	Mean	SD	Max.	Min.	Exceedance (%)[a)]
Beijing (BJ)	158.5	119.2	427.1	14.9	71
Tianjin (TJ)	136.1	91.2	398.9	13.4	72
Shijiazhuang (SJZ)	213.6	112.5	508.1	22.9	84
Xianghe (XH)	135.3	94	397.4	12.9	67
Xinglong (XL)	48.7	38.1	171.2	6.9	19
Yucheng (YC)	203.2	80.1	381.7	36.1	94
Wuxi (WX)	99.1	40.8	186.5	40.9	68
Hefei (HF)	119.2	43.4	222.1	37.2	81
Changsha (CS)	149.2	33.7	207.8	74.7	96
Qianyanzhou (QYZ)	77.5	26.8	134.6	24.2	55
Dinghushan (DHS)	59.6	23.4	99.6	20.2	32

a) Percentage of days on which daily $PM_{2.5}$ mass concentration exceeded the Grade II National Ambient Air Quality Standard (75 μg m^{-3}: GB3095-2012)

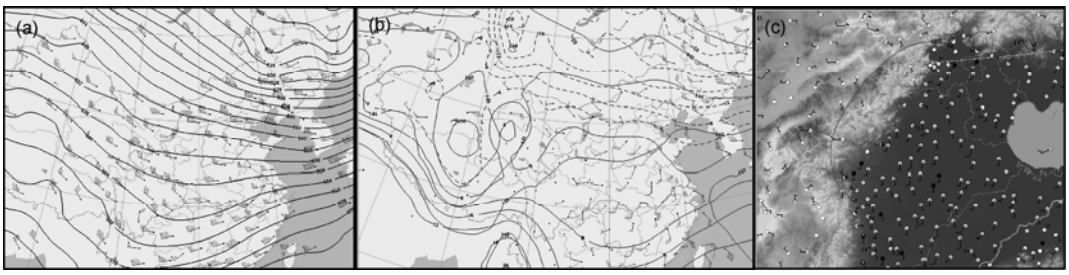

Figure 2 Synoptic maps on 12th January, 2013 for 500 hPa at 08 LT (a), 850 hPa at 20 LT (b), and surface at 08 LT (c).

scenario for a typical severe pollution day on 12 January. On this day, the circulation was remarkably zonal at 500 hPa over North China; the isobars were sparse at 850 hPa, and a south wind prevailed in the lower atmosphere. An inversion layer, caused by warm air advection, was present. A low pressure field was dominant in North China, and a wind convergence zone was set up along the plain-mountain transition area; a weak south wind prevailed over the piedmont plain in the Jing-Jin-Ji region. Thus, the pollutants in the south region were carried to the piedmont area by the wind, and the pollution accumulated and severe regional haze pollution developed.

2.2.2 *Meteorological conditions at the surface*

The temporal variations of the meteorological variables in Beijing, Tianjin and Shijiazhuang during January 2013 are depicted in Figure 3. Compared to a no-haze pollution episode, the characteristics of the surface meteorological variables during a severe haze pollution episode in North China were as follow: weak pressure (1027 hPa for a haze episode and 1032 hPa for a no-haze episode), weak pressure variation or lowering pressure during the accumulation period of the pollutants, higher temperature (–4.0°C for a haze episode and –5.5°C for a no-haze episode), higher relative humidity (72% for a haze episode and 51% for a no-haze episode), and a weak south wind (1.7 m s^{-1} for a haze episode and 2.4 m s^{-1} for a no-haze episode). Figure 3 illustrates that the increased relative humidity and sustained high relative humidity, the wind direction turning from north (clean air) to south (polluted air), and sustained weak winds were the primary meteorological causes for the accumulation, burst and preservation of haze pollution and the large-scale haze pollution over the Jing-Jin-Ji area.

2.2.3 *Atmospheric boundary layer*

Within the boundary layer, light south winds, temperature inversion, low mixed layer heights (less than 500 metres), and high humidity in the lower atmosphere (less than one kilometre) contributed to haze pollution over the Jing-Jin-Ji region. In the severe haze pollution episode, the inversion layer was as thick as 500–1000 metres, and the magnitude of the temperature inversion range was very large (5–10°C); in addition, advection inversion was notable in most areas. For example, on the 12th and 28th of January, the thickness of the inversion layer was over 600 m, the temperature range was over 8°C, and the mixed layer heights were approximately 200–300 m, which was one-tenth of the mixed layer heights (2000–3000 m) for a clear day (Figure 4). Thus, compared with the conditions of clean-air day, the diffusion space for pollutants was reduced ten times during the pollution event, which contributed to the accumulation of the local and regional pollutants. Meanwhile, the synergistic reaction of a variety of pollutants due to the higher humidity was the key cause of the rapid $PM_{2.5}$ increase.

2.2.4 *Dust superposition*

The surface monitoring data indicated that the particle concentrations were very high on the 12th and 13th of January over the Jing-Jin-Ji area. Satellite data analysis reveals that dust and polluted layers existed above the boundary layer over the Jing-Jin-Ji area; moreover, polluted continental aerosol, polluted dust, and smoke existed in the boundary layer on 12 January (Figure 5). Matrix backward trajectories revealed west upper air flow and slight south wind in the lower atmosphere (Figure 6). The results of the surface network monitoring indicated the hourly average values of the $PM_{2.5}$ concentrations reached maximums (250 and 260 μg m^{-3}) at Dunhuang and Shapotou, at 23:00 LT 11 January and 05:00 LT 12 January, respectively. Thus, the dust particles were carried into the Jing-Jin-Ji area by a northwest air flow, crossed the Taihang Mountains, and mixed with the local urban pollutants, which contributed to rare maximums of the hourly average values of the $PM_{2.5}$ concentrations (600–1000 μg m^{-3}), especially for Beijing, Shijiazhuang and Tianjin. Therefore, dust superposition was an import factor for the $PM_{2.5}$ to attain such high values.

2.3 Characteristics of haze pollution episodes and the formation mechanism

2.3.1 *Characteristics of haze pollution episodes*

Two primary types of haze pollution episodes were identified: one was characterised by the "explosive growth" of $PM_{2.5}$, which occurred in Haze Episode 2, and the other was characterized by the "sustained growth" of $PM_{2.5}$, which occurred in Haze Episode 5.

The variations in $PM_{2.5}$, PM_1, and the mass concentrations of the chemical compositions in PM_1 from 00:00 LT

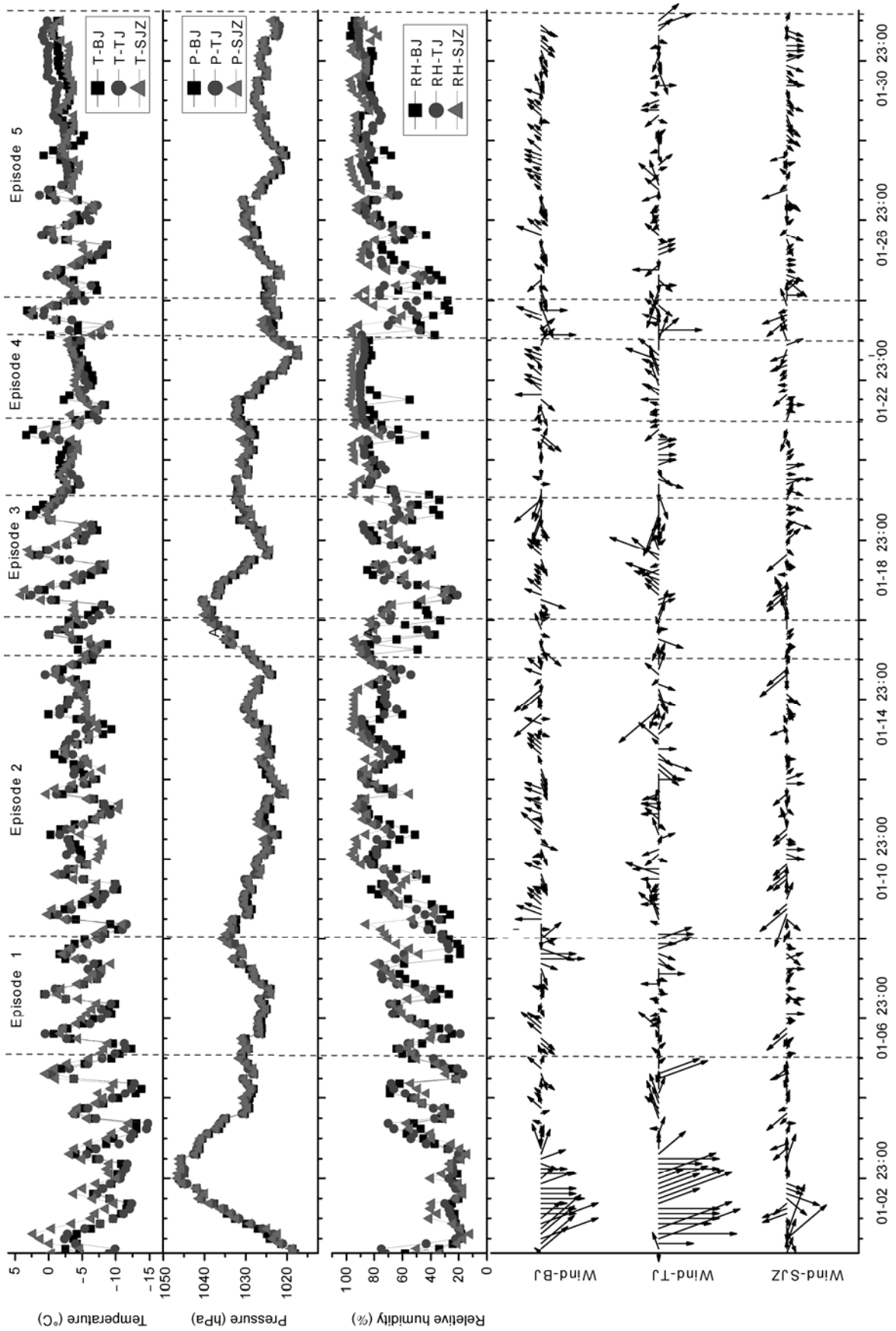

Figure 3 The temporal variation of the meteorological variables in Beijing, Tianjin and Shijiazhuang during January 2013, time interval is 3 hours.

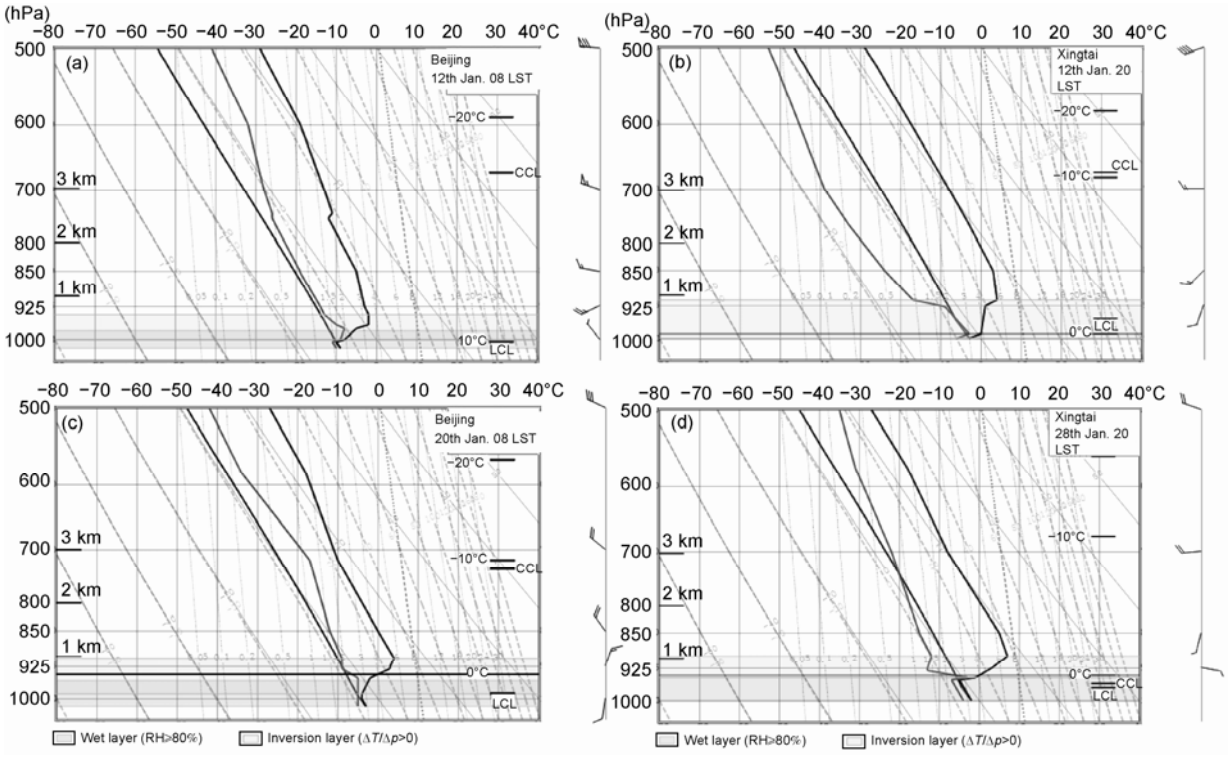

Figure 4 T-lnP diagram at Beijing and Xingtai on 12th and 28th January.

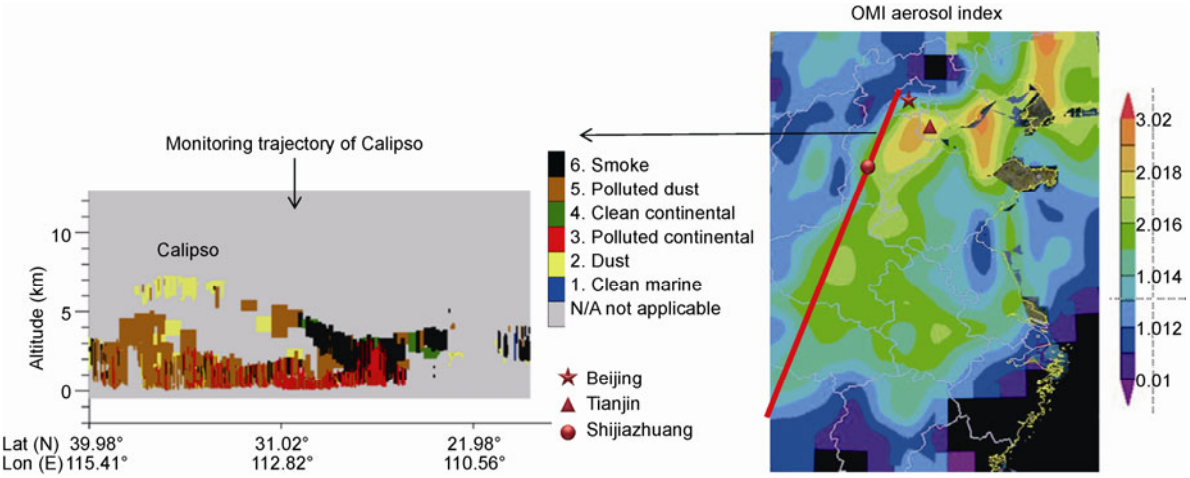

Figure 5 Results of satellite monitoring on 12th January.

12 January to 23:00 LT 14 January are displayed in Figure 7(a). The hourly average mass concentration of $PM_{2.5}$ increased quickly from a very low level (lower than 35 μg m^{-3}) to a very high level (higher than 500 μg m^{-3}) within eight hours. In this type of accumulating pollution episode, the growth rate of $PM_{2.5}$ was 88 μg m^{-3} h^{-1}, which is characterized as "explosive growth". Organic matter, sulphate and nitrate contributed the most to the increase of $PM_{2.5}$; the growth rates of these three aerosols were 19, 12 and 6 μg m^{-3} h^{-1}, respectively, the sum of which contributed to 90% of the PM_1 and 42% of the $PM_{2.5}$. The variations in $PM_{2.5}$, PM_1, and the mass concentrations of the chemical compositions in PM_1 from 00:00 LT 25 January to 23:00 LT 31 January are listed in Figure 7(b). The accumulation of $PM_{2.5}$ lasted nearly 100 hours, with a growth rate of 4 μg m^{-3} h^{-1}. Organic matter, sulphate and nitrate also exhibited sustained growth at the same time, with growth rates of 1.5, 0.9 and 0.7 μg m^{-3} h^{-1}, respectively, the sum of which contributed to 78% of the $PM_{2.5}$. To sum it up, an accumulating pollution episode of "explosive growth" displayed a very high level of fine particle mass concentration, but the high level only lasted a few hours. The accumulating pollution episode of "sustained growth" lasted much longer (a few days), and the peak of the $PM_{2.5}$ mass concentration was lower than

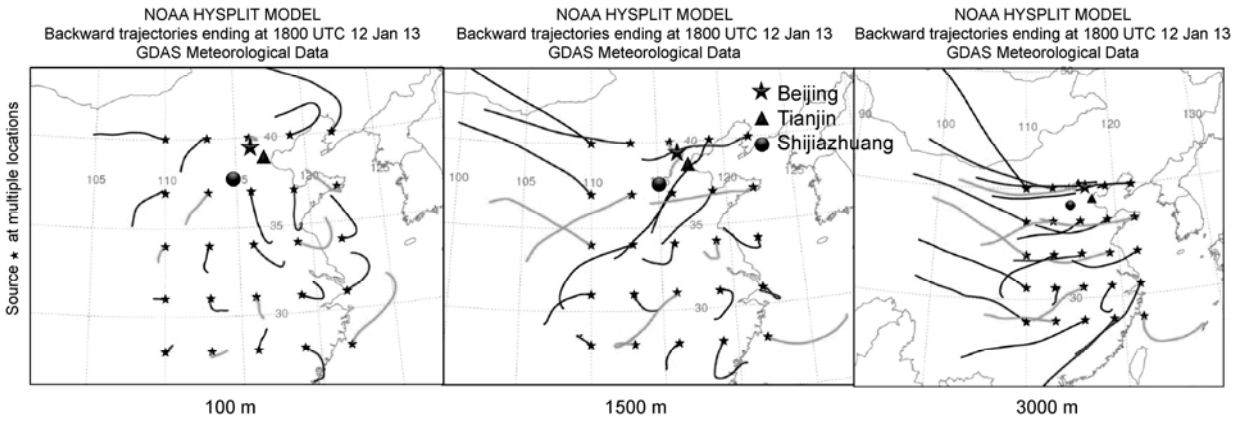

Figure 6 The 24-h matrix trajectories at 18 UTC 12 January for different altitudes.

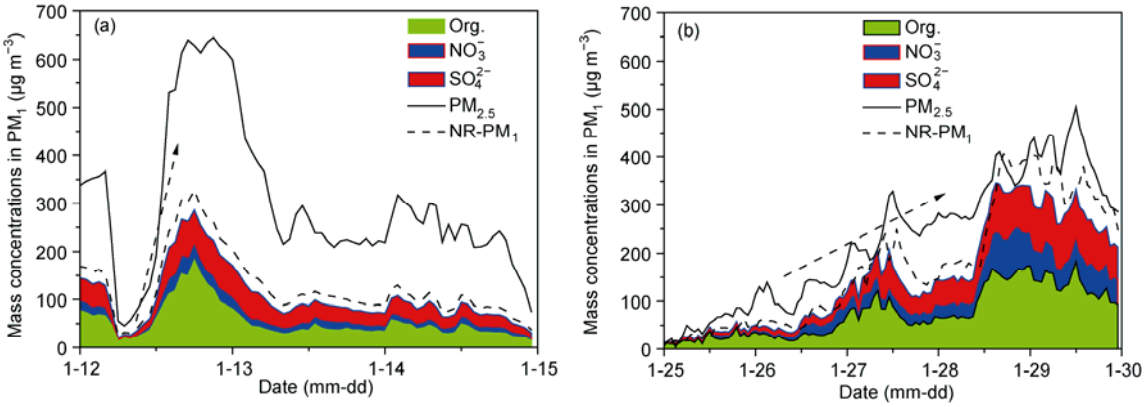

Figure 7 Variations of $PM_{2.5}$, PM_1 and mass concentrations of chemical compositions in PM_1 during haze episode. (a) Haze Episode 2; (b) Haze Episode 5.

that of the "explosive growth".

The average mass ratio of NR_PM_1/$PM_{2.5}$ was only 0.44 during Haze Episode 2, which suggests that the main contribution to the increase of $PM_{2.5}$ was $PM_{1–2.5}$. The average mass ratio of NR_PM_1/$PM_{2.5}$ was 0.70 during Haze Episode 5, which suggests that the main contribution to the increase of $PM_{2.5}$ was PM_1. Furthermore, both haze episodes had high mass ratios of $PM_{2.5}$/PM_{10} (0.67 for Haze Episode 2 and 0.69 for Haze Episode 5), which indicates that the main chemical compositions of $PM_{2.5}$ were NO_3^-, SO_4^{2-}, NH_4^+ and secondary organic matter (Chan and Yao, 2008). Consequently, the main contributor to $PM_{1\text{-}2.5}$ in Haze Episode 2 was secondary aerosols. The "droplet mode" of sulphate was observed to be in the size range of 0.56–1.0 μm or 1.0–1.8 μm at the PRD by Liu et al. (2008), and it was produced by aqueous-phase reactions or in-cloud processes. Similar results were also observed in our previous study conducted in Beijing; secondary inorganic ions showed higher concentrations during winter haze days, especially below the size of 1 μm (Huang, et al., 2013). Given the very high relative humidity (75%–95%) during Haze Episode 5, the secondary aerosols should be produced mainly by aqueous-phase reactions. In contrast, the relative humidity in Haze Episode 2 was much lower, especially in the accumulating pollution episode of "explosive growth" in which the relative humidity ranged from 50% to 75%; aqueous-phase reactions were suppressed, and the increased secondary aerosols of $PM_{1\text{-}2.5}$ were controlled likely by the heterogeneous reaction of gaseous pollutants (e.g., SO_2) on the surface of mineral particles. The mass ratio of NO_3^-/SO_4^{2-} has been used as an indication of the relative importance of mobile vs. stationary sources of sulphur and nitrogen in the atmosphere. Higher NO_3^-/SO_4^{2-} mass ratios indicate the predominance of mobile sources over stationary sources of pollutants (Arimoto et al., 1996). The average mass ratio of NO_3^-/SO_4^{2-} during the observation period was 0.73±0.33, which was much higher than the value measured during the winters of 2001–2003 in Beijing (i.e., 0.49). Wang et al. (2005) suggested that the contribution of mobile sources (e.g., motor vehicles) increased in Beijing, in accord with the adjustment of the energy structure in recent years. Furthermore, the mass ratio of NO_3^-/SO_4^{2-} in Haze Episode 2 (0.60±0.21) was much lower than that in Haze Episode 5 (0.73±0.33), which suggests a more significant contribution of mobile sources in the latter pollution episode.

2.3.2 *Cooperative transition*

According to the analysis of haze pollution characteristics, the haze pollution episodes during January 2013 were mainly caused by the fast secondary transformation of pri-

mary gaseous pollutants, such as SO_2 and NO_2, into secondary inorganic ions (sulphate and nitrate). To support this hypothesis, we plotted the correlations of ΔSO_2 versus ΔSO_4^{2-} in Figure 8(a) and the correlations of ΔNO_2 versus ΔNO_3^- in Figure 8(c). ΔSO_2 and ΔSO_4^{2-} are the mass concentrations after subtracting the background concentrations of SO_2 and SO_4^{2-}, i.e., 3.5 ppb and 0.7 μg m^{-3}, respectively. ΔNO_2 and ΔNO_3^- are the mass concentrations after subtracting the background concentrations of NO_2 and NO_3^-, i.e., 7.1 ppb and 0.1 μg m^{-3}, respectively. When RH is below 35%, ΔSO_2 and ΔSO_4^{2-} display a high correlation (R^2> 0.6) (Figure 8(b)), but the majority of SO_2 remains unoxidized. As RH increases, the concentration of ΔSO_2 decreases, and the concentration of ΔSO_4^{2-} increases accordingly. The correlation between ΔSO_2 and ΔSO_4^{2-} is sharply reduced when RH is over 50% (R^2<0.1), with most of the SO_2 being oxidized into sulphate. When RH is below 35%, the correlation between ΔNO_2 and ΔNO_3^- is lower than that observed in higher RH (20%–50%), which suggests that some NO_2 was oxidized into nitrate through a gas-phase reaction. The major process responsible for the oxidation of NO_2 into nitrate is the reaction of OH with NO_2 in the gas phase; this reaction leads to nitric acid, which is largely transferred to the aqueous phase, where it dissociates to form the nitrate anion. As RH further increases (>50%), the correlation between ΔNO_3^- and ΔNO_2 is sharply reduced (R^2<0.2), which suggests that most of the NO_2 has been oxidized into nitrate.

The Extend Aerosol Thermodynamics Model (E-AIM, Model II) with aerosol composition data (SO_4^{2-}, NO_3^- and NH_4^+) from HR-ToF-AMS measurements was used to predict the liquid water content (LWC) in this study (Clegg et al., 1998). When RH is below 50%, the LWC is rather low. However, a significant increase of the LWC was observed with increasing RH when RH>50%, which highlights the dominant role of aqueous-phase reactions to the secondary transformation of SO_2. The aqueous-phase oxidation of SO_2 can be very fast, and the oxidation rates depend on the fog droplet pH and oxidants (e.g., H_2O_2, O_3, and O_2/Fe/Mn) (Seinfeld and Pandis, 2006). Whereas H_2O_2 is the most important oxidant at a low pH (e.g., pH<5), O_3 is more important in the oxidation of SO_2 at a high pH (e.g., pH>5) (Shen et al., 2012). The calculated ion balances suggested a weak acid content for the observed aerosols (pH>5); therefore, O_3 could be the major contributor to the oxidation of SO_2. However, the O_3 concentration was very low during the observation period, especially in the haze pollution episodes (<15 μg m^{-3}). Such low O_3 levels cannot supply enough oxidizing capacity in the atmosphere; other oxidation reactions are likely responsible for the high level of sulphate during the observation period.

A few laboratory simulation studies have found that NO_2 and SO_2 have a synergistic effect when they react on the surface of mineral dust. Therefore, the formation of sulphate

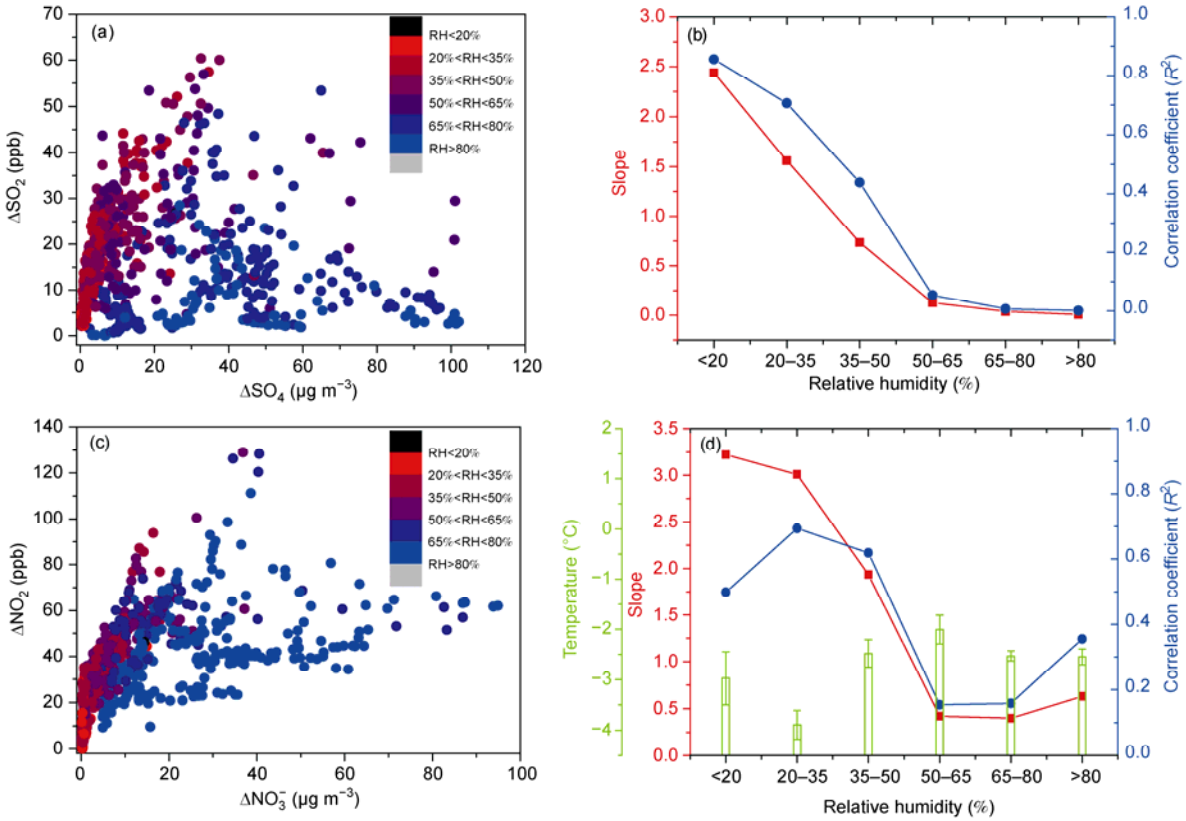

Figure 8 Scatter plots of (a) ΔSO_2 versus ΔSO_4^{2-} and (c) ΔNO_2 versus ΔNO_3^- at different RH ranges and (b) and (d) show the linear regression coefficient and slope as a function of RH.

from SO_2 was promoted by the coexistence of NO_2 (Ma et al., 2008; Liu et al., 2012). Metal ions (e.g., Fe/Mn) play important roles as catalysers in the process of oxidation. The reaction rate of sulphate increases in the presence of higher NO_2 concentrations (Martins et al., 2008). Another process that leads to the generation of sulphate is the reaction of HSO_3^- with peroxynitric acid ($HOONO_2$), which makes a sizable contribution to the formation of sulphate in the aqueous phase (Warneck, 1999). $HOONO_2$ is formed primarily by the gas-phase association of HO_2 and NO_2; it is then absorbed into the aqueous phase. In these two processes of sulphate production, NO_2 plays either a direct or indirect role in the generation of sulphate. Given that the average concentration of NO_2 was 45.4±19.8 ppb during the winter observation period, this value reached over 100 ppb during the haze episodes and reached the level of NO_2 in laboratory simulation studies. Consequently, we proposed that NO_2-catalyzed oxidation in the aqueous phase is a major pathway of sulphate formation in haze episodes. The relevant mechanism was based only on field observation data and cannot be validated through the chemical reaction mechanism model because some key radicals (e.g., OH and H_2O_2) were not observed in this study. Further research should focus on the observation of radicals, which would help demonstrate the catalytic mechanism of NO_2 in the secondary conversion of SO_2 to sulphate in field studies.

Another representation of cooperative transition was SO_2, NO_2, and the other primary gas pollutants transformed into secondary aerosols (e.g., sulphate and nitrate) through heterogeneous reactions of atmospheric particles, which can increase the size and mass concentrations of the particles. Figure 9 depicts the variation in the particle number size distribution and chemical compositions during Haze Episode 2. During the morning rush hours (06:00LT– 09:00LT), the particle number size distribution exhibited a major mode at 50 nm, which was attributed mainly to the carbon containing particles emitted by the motor vehicle exhaust emissions (Charron et al., 2003). Characterizing the haze pollution evolution, the particle size mode gradually increased to 100 nm at mid-day. As the particle size mode increased, the fractional contributions of secondary inorganic ions, such as sulphate and nitrate, also increased. The change in the composition of the particles enhances their hygroscopicity and increases the water adsorbed on a single particle. Moreover, the increased water content can accelerate the gas-liquid-solid reactions of SO_2 and NO_2 on particles, which leads to the increased hygroscopicity of the particles. Therefore, these processes form a positive feedback mechanism that enhances the conversion of primary gas pollutants to secondary aerosols. Consequently, it is more important to reduce the emissions of the precursor gases of $PM_{2.5}$ than those from primary emissions to reduce the $PM_{2.5}$ concentration in atmosphere. In central and eastern China, NO_x and SO_2 should be synchronously controlled to reduce the $PM_{2.5}$ concentration.

3 Conclusions

An intensive aerosol and trace gases campaign was conducted in central and eastern China in January 2013. The heaviest haze pollution days in the historical record of central and eastern China were identified, and the associated formation mechanism was analyzed in the Jing-Jin-Ji area. Five haze pollution episodes were identified based on daily fine particle mass concentrations in the most polluted area (Jing-Jin-Ji). Major cities in this area, such as Beijing, Tianjin and Shijiazhuang, all displayed consistency in the development and evolution of haze pollution. During the one month observation period, 70% of the daily $PM_{2.5}$ mass concentrations exceeded the Grade II standard (GB3095-2012); only less than 10% of the days met the Grade I standard. Distinct characteristics were observed among the five haze pollution episodes using a synergy of ground-based measurements, satellite and lidar observations. The characteristics of the haze pollution episodes and formation mechanisms were analyzed by observing the hourly changes of $PM_{2.5}$ aerosols and their chemical compositions in Beijing, a city in the Jing-Jin-Ji area.

The major findings of this study can be summarized as

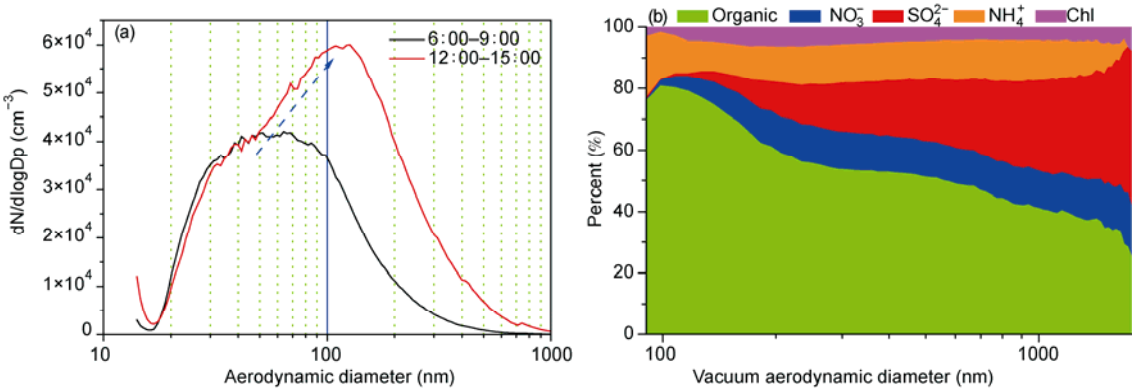

Figure 9 Particle number size distributions and fractional contributions of organics, nitrate, sulfate, ammonium and chloride to the PM_1 mass during the haze episode from 6:00LT to 15:00LT, 12 January.

follows:

(1) Atmospheric circulation, local meteorological factors, and the structure of the boundary layer, together with specific geographical conditions, were unfavourable for pollutant diffusion. Strong cold air events were sparse, and the weather systems were weak in central and eastern China. Zonal upper air circulation was dominant over North China, and warm air advection existed in the lower atmosphere; in addition, a low or weak pressure field was dominant over North China, which did not favour dispersion. Increasing humidity and sustained high humidity conditions, the wind direction turning from north to south and sustained weak wind were the main meteorological causes for the severe haze pollution over the Jing-Jin-Ji area. Meanwhile, the pollutants were concentrated at the surface layer due to the intense, thick inversion layer and low mixed layer height.

(2) The abnormally high amount of NO_x during the haze episodes, produced by fossil fuel combustion and vehicle emissions, played either a direct or indirect role in the rapid secondary transformation of SO_2 into sulphate aerosols. SO_2, NO_2, and the other primary gas pollutants were transformed into secondary aerosols (e.g., sulphate and nitrate) through heterogeneous reactions on the surface of carbon-containing ultrafine particles; the change in the composition of the particles enhances their hygroscopicity and increases the size and mass concentrations of the ultrafine particles.

(3) As haze pollution becomes a regional atmospheric pollution problem, synchronous emission abatement policies that are based on integrated planning should be implemented in stages to improve the regional air quality throughout central and eastern China, especially for the Jing-Jin-Ji area. Among these abatement policies, stricter single pollutant emission standards and further emission reductions are of particular importance to reduce the synergistic effects between various pollutants.

This work was supported by the Chinese Academy of Sciences Strategic Priority Research Program (Grant Nos. XDB05020000 and XDA05100100) and the National Natural Science Foundation of China (Grant Nos. 41230642 and 41021004). The authors thank Yuepeng Pan, Tao Song, Tianxue Wen, Yinghong Wang, Fangkun Wu, Mengtian Cheng and other teammates for their sincere help with the data analysis and collection. We also thank the staff of Xinghe, Tianjin, Shijiazhuang, Xinglong, Yucheng, Wuxi, Hefei, Changsha, Qianyanzhou and Dinghushan in the CARE-China network for their cooperation. We are grateful to all of the observers, maintainers and analysts for their hard work.

Arimoto R, Duce R A, Savoie D L, et al. 1996. Relationships among aerosol constituents from Asia and the North Pacific during PEM-West A. J Geophys Res, 101: 2011–2023

Canagaratna M R, Jayne J T, Jimenez J L, et al. 2007. Chemical and microphysical characterization of ambient aerosols with the aerodyne aerosol mass spectrometer. Mass Spectrom Rev, 26: 185–222

Chan C K, Yao X H. 2008. Air pollution in mega cities in China. Atmos Environ, 42: 1–42

Chang D, Song Y, Liu B. 2009. Visibility trends in six megacities in China 1973–2007. Atmos Res, 94: 161–167

Charron A, Harrison R M. 2003. Primary particle formation from vehicle emissions during exhaust dilution in the roadside atmosphere. Atmos Environ, 37: 4109–4119

Che H Z, Zhang X Y, Li Y, et al. 2009. Haze trends over the capital cities of 31 provinces in China, 1981–2005. Theor Appl Climatol, 97: 235–242

China National Environmental Monitoring Center. 2006. Automated Methods for Ambient Air Quality Monitoring. http://www.cnemc.cn/resource/crm/newImages/7b22f778-964f-4be6-99de-41be74c7900f.pdf

Clegg S L, Brimblecombe P, Wexler A S. 1998. A thermodynamic model of the system H^+-NH_4^+-SO_4^{2-}-NO_3^--H_2O at tropospheric temperatures. J Phys Chem, 102: 2137–2154

DeCarlo P F, Kimmel J R, Trimborn A, et al. 2006. Field-deployable, high-resolution, time-of-flight aerosol mass spectrometer. Anal Chem, 78: 8281–8289

Department of Energy Statistics, National Bureau of Statistics of China. 2001. China Energy Statistical Yearbook 2001. Beijing: China Statistics Press

Department of Energy Statistics, National Bureau of Statistics of China. 2011. China Energy Statistical Yearbook 2011. Beijing: China Statistics Press

Ding J, Zhu T. 2003. Heterogeneous reactions on the surface of fine particles in the atmosphere. Chin Sci Bull, 48: 2267–2276

Huang Y M, Liu Z R, Chen H, et al. 2013. Characteristics of mass size distributions of water-soluble inorganic ions during summer and winter haze days of Beijing (in Chinese). Environ Sci, 34: 1236–1244

Liu C, Ma Q, Liu Y, et al. 2012. Synergistic reaction between SO_2 and NO_2 on mineral oxides: A potential formation pathway of sulfate aerosol. Phys Chem Chem Phys, 14: 1668–1676

Liu S, Hu M, Slanina S, et al. 2008. Size distribution and source analysis of ionic compositions of aerosols in polluted periods at Xinken in Pearl River Delta (PRD) of China. Atmos Environ, 42: 6284–6295

Ma Q X, Liu Y C, He H. 2008. Synergistic effect between NO_2 and SO_2 in their adsorption and reaction on gamma-alumina. J Phys Chem A, 112: 6630–6635

Martins C R, Alves J J, Carvalho W B, et al. 2008. Influence of NO_2 and metal ions on oxidation of aqueous-phase S(IV) in atmospheric concentrations. An Acad Bras Cienc, 80: 279–290

Parrish D D, Zhu T. 2009. Clean air for megacities. Science, 326: 674–675

Patashnick H, Rupprecht E. 1991. Continuous PM_{10} measurements using the tapered element oscillating microbalance. J Air Waste Manage Assoc, 41: 1079–1083

Seinfeld J H, Pandis S N. 2006. Atmospheric Chemistry and Physics: From Air Pollution to Climate Change. 2nd ed. New York: Wiley, John & Sons, Incorporated. 1203

Shen X, Lee T, Guo J, et al. 2012. Aqueous phase sulfate production in clouds in eastern China. Atmos Environ, 62: 502–511

Sullivan R, Guazzotti S, Sodeman D, et al. 2007. Direct observations of the atmospheric processing of Asian mineral dust. Atmos Chem Phys, 7: 1213–1236

Usher C R, Michel A E, Grassian V H. 2003. Reactions on mineral dust. Chem Rev, 103: 4883–4940

Wang Y, Zhuang G S, Tang A H, et al. 2005. The ion chemistry and the source of $PM_{2.5}$ aerosol in Beijing. Atmos Environ, 39: 3771–3784

Warneck P. 1999. The relative importance of various pathways for the oxidation of sulfur dioxide and nitrogen dioxide in sunlit continental fair weather clouds. Phys Chem Chem Phys, 1: 5471–5483

Xin J Y, Wang Y S, Wang L L, et al. 2012. Reductions of $PM_{2.5}$ in Beijing-Tianjin-Hebei urban agglomerations during the 2008 Olympic Games. Adv Atmos Sci, 29: 1330–1342

Zhang X, Gong S, Shen Z, et al. 2003. Characterization of soil dust aerosol in China and its transport and distribution during 2001 ACE-Asia 1. Network observations. J Geophys Res, 108: 8032–8039

Zhang Y H, Hu M, Zhong L J, et al. 2008. Regional integrated experiments on air quality over Pearl River Delta 2004 (PRIDE-PRD2004): Overview. Atmos Environ, 42: 6157–6173

Zhu T, Shang J, Zhao D F. 2010. The roles of heterogeneous chemical processes in the formation of an air pollution complex and gray haze. Sci China Chem, 40: 1731–1740

Zhu T. 2005. Air Pollution Complex at Urban and Regional Scales, Progress in Environmental Chemistry (in Chinese). Beijing: Chemical Industry Press